# Dynamic Motion Planning for the Design of Robotic Gait Rehabilitation

**Chia-Yu E. Wang**

**James E. Bobrow**
e-mail: jebobrow@uci.edu

**David J. Reinkensmeyer**[1]
e-mail: dreinken@uci.edu

Department of Mechanical and Aerospace Engineering,
University of California, Irvine, California 92679

*In this paper we examine a method to control the stepping motion of a paralyzed person suspended over a treadmill using a robot attached to the pelvis. A leg swing motion is created by moving the pelvis without contact with the legs. The problem is formulated as an optimal control problem for an underactuated articulated chain. The optimal control problem is converted into a discrete parameter optimization and an efficient gradient-based algorithm is used to solve it. Motion capture data from an unimpaired human subject is compared to the simulation results from the dynamic motion optimization. Our results suggest that it is feasible to drive repetitive stepping on a treadmill by a paralyzed person by assisting in torso movement alone. The optimized, pelvic motion strategies are comparable to "hip-hiking" gait strategies used by people with lower limb prostheses or hemiparesis. The resulting motions can be found at the web site http://www.eng.uci.edu/~chwang/project/stepper/stepper.html.* [DOI: 10.1115/1.1979507]



## 1 Introduction

In the U.S. alone, over 700,000 people experience a stroke each year, and over 10,000 people experience a traumatic spinal cord injury. Impairment in walking ability after such neurologic injuries is common. Recently, a new approach to locomotion rehabilitation called step training with body weight support on a treadmill (BWST) has shown promise in improving locomotion after stroke and spinal cord injury [1]. The technique involves suspending the patient in a harness above a treadmill in order to partially relieve the weight of the body, and manually assisting the legs and pelvis in moving in a walking pattern (Fig. 1). Patients who receive this therapy can significantly increase their independent walking ability and overground walking speed [3]. It is hypothesized that the technique works in part by stimulating remaining force, position, and touch sensors in the legs during stepping in a repetitive manner, and that residual circuits in the nervous system learn from this sensor input to generate motor output appropriate for stepping.

Patient access to step training with BWST is currently limited because the training is labor intensive. Multiple therapists are often required to control the pelvis and legs, and the therapists quickly fatigue while assisting in movement. Several research groups are pursuing robotic implementations of the technique in an attempt to make it less labor intensive, more consistent, and more widely accessible [4–7]. Implementing the technique with robotics is also attractive because it could improve experimental control over the training, thus providing a means to better understand and optimize its effects.

A difficulty in automating step training with BWST is that the required patterns of forces at the pelvis and legs are unknown. For example, the relative importance of assisting at the pelvis and legs is unclear. One approach toward determining the required forces is to instrument the therapists' hands with force and position transducers [8]. However, therapists are relatively limited in the forces that they can apply compared to robots, and there is no guarantee that any given therapist has selected an optimal solution. Current robotic devices for step training with BWST have taken the simplified approach of replicating leg kinematics, and moving the torso in a gait-like up and down pattern [5,6].

In this paper we explore an alternate approach toward generating strategies for assisting in gait training: dynamic motion optimization. Dynamic motion optimization provides a formalized method for determining motions for underconstrained tasks, and may reveal novel strategies for achieving the tasks. It has been used with success to simulate human control over such activities as diving, jumping, and walking [9–13]. The objective of this study was to use dynamic motion optimization to determine to what extent repetitive stepping by a paralyzed patient can theoretically be generated by assisting in pelvis motion alone. Portions of this work have been published in conference paper format [14].

## 2 Methods

**2.1 Human Model and Walking Motion.** For studying the motion of the legs, the head, arms, torso (HAT), and pelvis were combined into a single rigid body. We assumed that the walking gait cycle was bilaterally symmetric. That is, in the gait cycle, the right-side stance and swing phases were assumed to be identical to the left-side stance and swing phases, respectively. Based on this assumption, only one-half of the gait cycle was simulated. We refer to the joints on the side of the stance phase as the stance joints and the joints on the side of the swing phase as the swing joints.

The stance hip was modeled as a ball joint, with its position with respect to an inertial reference frame assumed to equal measured data. This could be achieved by using a robot to translate the stance hip along the normative, measured kinematic trajectory. From the stance hip joint position, we assumed that a robot could rotate the HAT and pelvis about the $x$ (lateral pelvic tilt) and $y$ (swivel) axes of rotation, but not the $z$ (forward pelvic tilt) axis (refer to Fig. 2). By using these two rotational degrees of freedom (DOF), rather than three, for the pelvis, we have constrained the pelvic rotation about the $z$ axis to be zero. This assumption is justified because forward/backward trunk tilt is relatively small (less than 5 deg) during normal walking [15], and patients are suspended from a harness during body weight supported locomotor training (Fig. 1), thereby further constraining pelvis/torso tilt and making it difficult to actively control. The swing hip was modeled as a three DOF ball joint rotating about axes in the $x$ (hip adduction/abduction), $y$ (hip internal/external rotation), and $z$ (hip flexion/extension) directions. The knee and ankle were modeled as one DOF hinge joints about the $z$ axis (knee extension/flexion and

[1]Also at: Center for Biomedical Engineering, University of California, Irvine, California 92679.

Contributed by the Journal of Biomechanical Engineering. Manuscript received: March 27, 2002; revision received: May 28, 2004. Associated Editor: Marcus Pandy

  

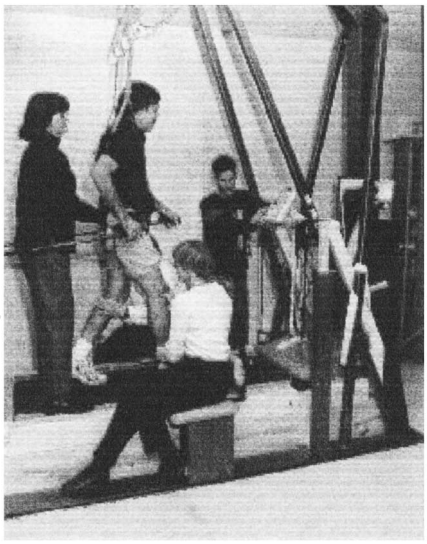

**Fig. 1 Step training with body weight support on a treadmill. Two therapists assist in leg movement, while a third assists in torso movement. Reprinted from A. Behrman and S. Harkema [2], with permission of the American Physical Therapy Association.**

ankle dorsal/plantar flexion, respectively).

Motion capture data of key body segments for an unimpaired subject during treadmill walking was obtained using a video-based system (Motion Analysis Corp.) at the Department of Veterans Affairs Medical Center, Long Beach, CA. The sampling rate of motion capture was 60 Hz. The treadmill speed was selected to be 1.25 m/sec to approximate a speed commonly used in step training with BWST [2]. External markers were attached to the subject at the antero-superior iliac spines (ASISs), knees, ankles, tops of the toes, and backs of the heels. The hip joint center location was estimated from the right and left ASIS's based on Bell's method [16], with a small correction suggested by [17]. From the two ASIS locations the pelvic swivel and lateral tilt was computed. Note that a third marker was not needed on the pelvis to obtain its orientation since we assumed that the forward/backward pelvic tilt was zero.

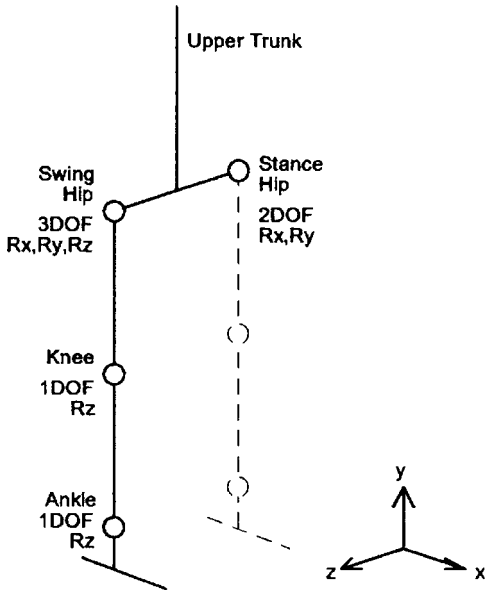


**Fig. 2 Human model**

**Table 1 Link lengths. $l_{Hip}$=distance between the right and left hip joint center locations; $l_{U\ Leg}$ and $l_{L\ Leg}$=lengths of upper and lower legs, respectively; $l_{Foot}$=the vertical distance between the ankle and sole of the foot, assuming the subject stands straight up; $l_{Toe}$=the horizontal distance between the ankle and toes; $l_{Heel}$=the horizontal distance between the ankle and heel.**

| $l_{Hip}$ | $l_{U\ Leg}$ | $l_{L\ Leg}$ | $l_{Foot}$ | $l_{Toe}$ | $l_{Heel}$ |
|---|---|---|---|---|---|
| 0.146 m | 0.470 m | 0.489 m | 0.079 m | 0.175 m | 0.069 m |

One representative step with a duration of 0.5 sec was chosen for comparison with the optimization results described in the following sections. The step was chosen arbitrarily from approximately one hundred recorded steps, but fell within the variability of these steps. A least-squares method was used to convert the positions of the markers to the link lengths and joint angles based on the forward kinematics of the model described above. The resulting link lengths are shown in Table 1. The human subject was 1.95 m tall and weighed 75 kg. Dynamic properties of the body segments were estimated using regression equations based on segment kinematic measurements (Table 2) [18].

Passive torque-angle properties of the hip, knee, and ankle joints were measured for the subject with a motorized dynamometer (Biodex Inc.). The dynamometer imposed slow isovelocity movements at the joints and measured applied torques and resulting joint angles. Joints were measured in a gravity-eliminated configuration, or, if not possible, torques due to gravity were estimated and subtracted. We modeled the joints as nonlinear springs in which the joint torque was a polynomial function of the joint angle. A least-squares method was used to obtain the best-fit polynomial of order 3 for the torque-angle properties of each of the joints except for the ankle joint. A polynomial of order 7 provided a better fit to the ankle joint data (Fig. 3). Define $\tau_m$ as the measured joint torque and $q$ as the corresponding joint angle, the resulting polynomial curves were:

**Table 2 Dynamic properties of the human model, estimated using regression equations based on segment kinematic measurements [18]**

| Link | Mass (kg) | Inertia (kg m$^2$) | Center of mass (m) |
|---|---|---|---|
| Upper Trunk | 46.0704 | $\begin{bmatrix} 3.2288 & 0 & 0 \\ 0 & 0.7783 & 0 \\ 0 & 0 & 2.7573 \end{bmatrix}$ | $\begin{bmatrix} -0.0009 \\ 0.3600 \\ 0 \end{bmatrix}$ |
| Upper Leg | 9.5368 | $\begin{bmatrix} 0.1574 & 0 & 0 \\ 0 & 0.0353 & 0 \\ 0 & 0 & 0.1535 \end{bmatrix}$ | $\begin{bmatrix} -0.0240 \\ -0.1700 \\ 0.0070 \end{bmatrix}$ |
| Lower Leg | 3.5586 | $\begin{bmatrix} 0.0638 & 0 & 0 \\ 0 & 0.0055 & 0 \\ 0 & 0 & 0.0624 \end{bmatrix}$ | $\begin{bmatrix} -0.0050 \\ -0.2073 \\ 0.0190 \end{bmatrix}$ |
| Foot | 1.4373 | $\begin{bmatrix} 0.0028 & 0 & 0 \\ 0 & 0.0088 & 0 \\ 0 & 0 & 0.0070 \end{bmatrix}$ | $\begin{bmatrix} 0.0440 \\ -0.0394 \\ 0.0090 \end{bmatrix}$ |

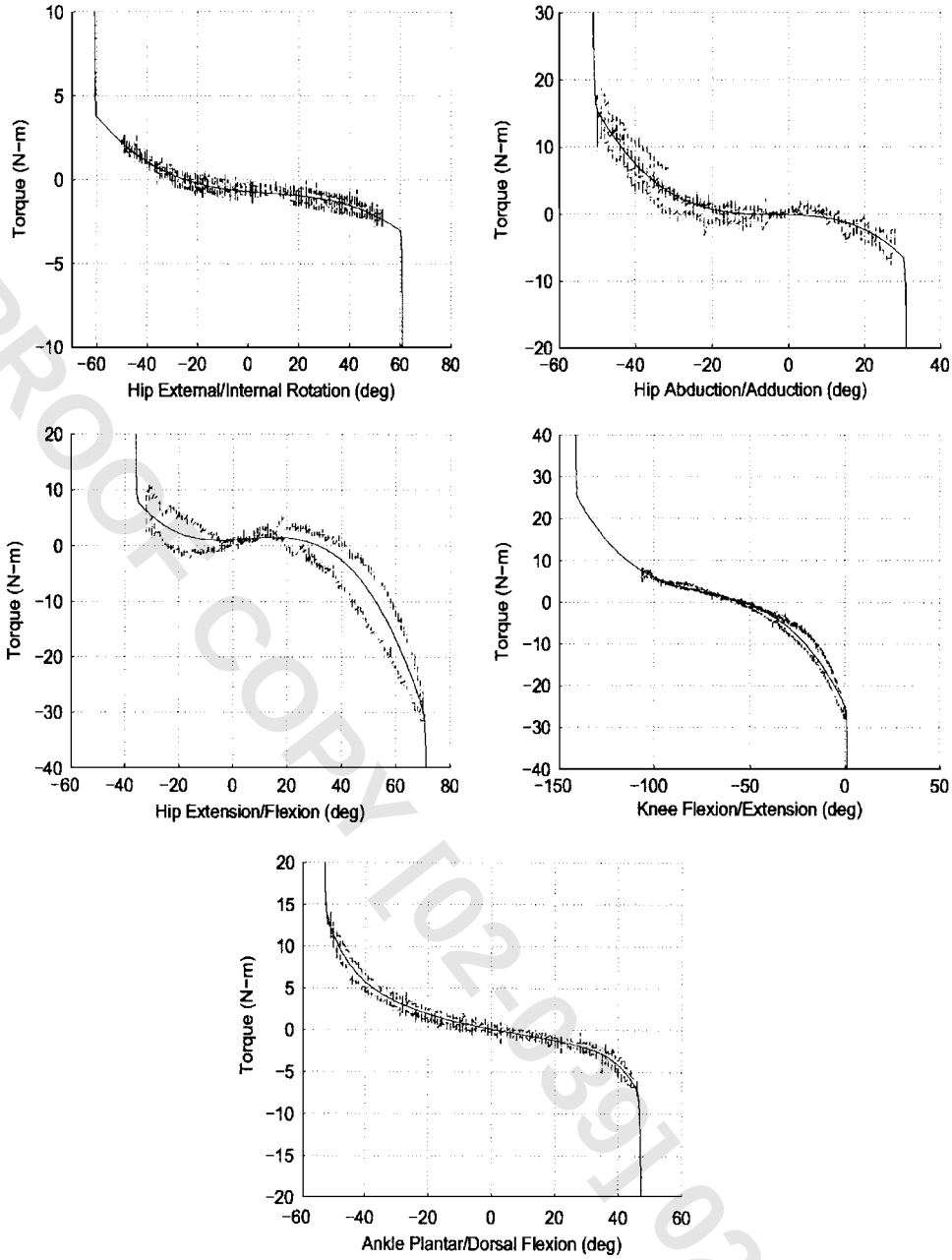


**Fig. 3 Measured passive torque-angle relationships ($\tau_{st}$) incorporated into the model**

- Hip External/Internal Rotation $(-60°, 60°)$

$$\tau_m = -0.6837 - 0.7621q + 0.9772q^2 - 2.2620q^3 \quad (1)$$

- Hip Abduction/Adduction $(-50°, 30°)$

$$\tau_m = -0.0542 - 0.8266q - 6.0205q^2 - 29.0271q^3 \quad (2)$$

- Hip Extension/Flexion $(-35°, 70°)$

$$\tau_m = 1.0863 + 1.5721q + 6.3488q^2 - 23.0405q^3 \quad (3)$$

- Knee Flexion/Extension $(-140°, 0°)$

$$\tau_m = -24.9343 - 53.1584q - 37.5211q^2 - 9.8685q^3 \quad (4)$$

- Ankle Plantar/Dorsal Flexion $(-52°, 46°)$

$$\tau_m = 0.1305 - 3.9956q + 1.5596q^2 - 4.7881q^3 \quad (5)$$

$$+ 2.4229q^4 + 6.2372q^5 - 5.6802q^6 - 19.5304q^7 \quad (6)$$

[The joint lower and upper bounds, $\underline{q}$ and $\overline{q}$, are shown in the parentheses $(\underline{q}, \overline{q})$.]

In addition to the polynomial function, a nonlinear spring-damper torque $\tau_{sd}$ was used to place a firm limit on joint movement at its upper and lower bounds.

$$\tau_{sd} = \begin{cases} -\beta\{10^4(q-\overline{q}) + 5 \times 10^2\dot{q}\} & \text{if } q \geqslant \overline{q} \\ -\beta\{10^4(q-\underline{q}) + 5 \times 10^2\dot{q}\} & \text{if } q \leqslant \underline{q} \\ 0 & \text{otherwise} \end{cases} \quad (7)$$

where

$$\beta = \begin{cases} 6\times 10^5(q-\bar{q})^5 - 1.5\times 10^5(q-\bar{q})^4 + 10^4(q-\bar{q})^3 & \text{if } \bar{q}+0.1 \geqslant q \geqslant \bar{q} \\ -6\times 10^5(q-\underline{q})^5 - 1.5\times 10^5(q-\underline{q})^4 - 10^4(q-\underline{q})^3 & \text{if } \underline{q}-0.1 \leqslant q \leqslant \underline{q} \\ 1 & \text{otherwise} \end{cases} \tag{8}$$

The function $\tau_{sd}$ was selected to be $C^2$ continuous in order to be used in the computation of the analytical gradient in the dynamic motion optimization. The resulting model for the torque contribution from the soft tissue $\tau_{st}$ for each joint has the form $\tau_{st}=\tau_m+\tau_{sd}$ with $\dot{q}=0$, are shown as a solid line crossing the experimental data in Fig. 3.

**2.2 Formulation of the Optimal Control Problem.** The objective of this study was to explore to what extent repetitive stepping by a paralyzed patient can theoretically be generated by moving the pelvis along some trajectory, without explicitly controlling the legs. That is, could a normal gait be generated by a robot that maneuvers the pelvis without requiring robots that maneuver the legs? We assumed that the robot was capable of moving the pelvis such that the stance hip moved along a normal, unimpaired trajectory, while simultaneously lifting the swing hip to control movement of the swing leg. In other words, our strategy is to control the motion of the stance leg along a normative trajectory using a position-controlled robotic device. With a reasonably stiff controller, the stance leg motion would not be influenced by the torques applied to the stance hip, and thus the problem of swing control can be addressed in isolation. We also assumed that the robot-assisted motion was initiated when the treadmill had pulled the stance leg backward to the position from which the swing would normally be initiated, with the foot's horizontal and vertical velocity equal to zero. The robot-generated motion then initiated the transition from stance to swing, driving the leg toward the desired foot-fall location. We modeled the swing leg as a paralyzed (i.e., unactuated) linkage with the identified passive torque-angle properties.

This problem can be addressed mathematically as an optimal control problem for an underactuated system. We are interested in obtaining a normal swing phase of the paralyzed leg, starting with the leg in an extended position with zero initial joint velocities by shifting the pelvis. We used the motion of the stance hip found from the video capture data of the unimpaired subject as an input to our underactuated human model. Specifically, the stance hip joint center locations were approximated using B-spline curves based on the motion capture data. The degrees of freedom of the human model are shown in Table 3. $S_{rx}$, $S_{ry}$, and $S_{rz}$ represent screw axes of rotation about the $x$, $y$, and $z$ axes, respectively; $S_{tx}$, $S_{ty}$, and $S_{tz}$ screw axes of translation along the $x$, $y$, and $z$ axes, respectively; and the joint positions $q_i$'s corresponded sequentially to the screw axes. We considered the swing motion to be an optimal control problem as follows: Minimize $\tau(t)$ subject to

$$J = \frac{1}{2}\int_0^{t_f}\sum_{i=4}^{10} w_{ei}\tau_i^2 dt + J_p(q,\dot{q}) \tag{9}$$

$$H(q)(\ddot{q}) + h(q,\dot{q}) = \tau + \tau_{st} \tag{10}$$

$$q(0) = q_0, \quad \dot{q}(0) = \dot{q}_0 \tag{11}$$

**Table 3 DOF of the human model**

| Joint | Stance hip | | Swing hip | Knee | Ankle |
|---|---|---|---|---|---|
| DOF | 3 | 2 | 3 | 1 | 1 |
| Screw axis | $S_{tx}$, $S_{ty}$, $S_{tz}$ | $S_{ry}$, $S_{rx}$ | $S_{rx}$, $S_{ry}$, $S_{rz}$ | $S_{rz}$ | $S_{rz}$ |
| Joint position | $q_1$, $q_2$, $q_3$ | $q_4$, $q_5$ | $q_6$, $q_7$, $q_8$ | $q_9$ | $q_{10}$ |

$$q(t_f) = q_f, \quad \dot{q}(t_f) = \dot{q}_f \tag{12}$$

where Eq. (10) represents the dynamics for the human model with joint coordinates $q \in \Re^{10}$, active applied joint torques $\tau \in \Re^{10}$, and measured passive torques due to soft tissue stiffness $\tau_{st} \in \Re^{10}$. $H(q)$ is the generalized mass matrix and $h(q,\dot{q})$ contains the centrifugal, Coriolis, and gravitational forces. $\tau_1$, $\tau_2$, and $\tau_3$ are the generalized forces associated with the translation of the stance hip (and are not included in the cost function since the position of the stance hip was specified by the motion capture data); $\tau_4$ and $\tau_5$ are the moments corresponding to the two rotations of the stance hip (controlled by the robot); $\tau_6$, $\tau_7$, and $\tau_8$ are the swing hip moments (corresponding to hip abduction/adduction, external/internal rotation, and extension/flexion, respectively); $\tau_9$ and $\tau_{10}$ correspond to knee and ankle rotation moments, respectively; and $w_{ei}$'s are positive weighting coefficients. $\tau_6 \sim \tau_{10}$ were assumed zero for the impaired leg. $\tau_{st4} \sim \tau_{st10}$ were modeled as nonlinear spring-damper systems to capture the passive torque-angle properties of the joints, as described above, while $\tau_{st1} \sim \tau_{st3}$ were zero since no muscular force was needed for the linear translation of the stance hip (i.e., the robot was assumed to control these degrees of freedom). Equations (11) and (12) define the initial and final joint velocities of the swing leg, selected so that swing starts and ends at the same position and velocity as an unimpaired subject, as explained in the preceding paragraph.

The term $J_p(q,\dot{q})$ in Eq. (9) is a penalty function used to avoid collision of the swing leg with the stance leg and the ground and to achieve the final desired position. It is the sum of three terms, $J_p(q,\dot{q})=J_{p1}+J_{p2}+J_{p3}$, where $J_{p1}$ and $J_{p2}$ are two functions introduced to penalize the penetration of the swing leg with the stance leg and the ground, and $J_{p3}$ is used to drive the swing leg to the desired final configuration. In order to obtain the collision penalty functions $J_{p1}$ and $J_{p2}$, note that since the position of the stance hip in the $z$ direction was less than that of the swing hip in the selected coordinate system (Fig. 2), the following was added to the cost function. Let $(\cdot)_+$ be a function that is positive when its argument is positive and zero otherwise. The penalty functions are then

$$J_{p1} = \sum_{i=0}^{n_t} w_{p1}\left\{\left[y_{ground} - y_{heel}\left(\frac{i}{n_t}t_f\right)\right]_+^2 + \left[y_{ground} - y_{toe}\left(\frac{i}{n_t}t_f\right)\right]_+^2\right\} \tag{13}$$

$$J_{p2} = \sum_{i=0}^{n_t} w_{p2}\left\{\left[z_1\left(\frac{i}{n_t}t_f\right) - z_{knee}\left(\frac{i}{n_t}t_f\right)\right]_+^2 + \left[z_2\left(\frac{i}{n_t}t_f\right) - z_{heel}\left(\frac{i}{n_t}t_f\right)\right]_+^2\right\} \tag{14}$$

■■ (15)

where $n_t > 0$ is the number of time instances when the collision is checked, and was set to be 50; $w_{p1}$ and $w_{p2}$ are positive weighting coefficients; and $(x,y,z)_{knee}$, $(x,y,z)_{heel}$, and $(x,y,z)_{toe}$ are the Cartesian coordinates of the swing knee, heel, and toes, respectively, which were computed using the forward kinematics. $y_{ground}$ is the position of the ground in the $y$ direction, which is equal to the position of the toes of the swing leg at the beginning of the gait cycle. $z_1$ and $z_2$ are selected to constrain the movement of the

swing leg in the $z$ direction to avoid excessive out of plane motion.

The following cost function was used to drive the passive joints of the swing leg to the desired final configuration:

$$J_{p3} = \frac{1}{2}\sum_{ip} w_{p31}[q_{ip}(t_f) - q_{fip}]^2 + w_{p32}[\dot{q}_{ip}(t_f) = \dot{q}_{fip}]^2 \quad (16)$$

where $ip$ is the passive joint index; $q_{fip}$ and $\dot{q}_{fip}$ the final joint position and velocity, respectively; and $w_{p31}$ and $w_{p32}$ the weighting coefficients.

**2.3 Dynamic Motion Optimization via Direct Parameter Optimization.** In order to formulate the optimal control problem for a numerical solution, the joint trajectories were interpolated by uniform, $C^4$ continuous quintic B-spline polynomials over the knot space of an ordered time sequence (see also [19–22]). Let the knot sequence be $0=t_0=\cdots=t_5\leqslant t_6\leqslant\cdots\leqslant t_m\leqslant t_{m+1}=\cdots=t_{m+6}=t_f$ with $m\geqslant 5$ and $\Delta t=t_j-t_{j-1}=t_f/(m-4)$ for $j=6,7,\ldots,m+1$. Let $n_a$ be the number of actuated joints. The joint trajectories for these joints, $q_a\in\Re^{n_a}$, are then written as

$$q_a(t,P) = \sum_{j=0}^{m} p^j B_{j,6}(t) \quad (17)$$

where $P=\{p^0,\ldots,p^m\}$ with $p^j\in\Re^{n_a}$ is the set of the control points; and $B_{j,6}$ is a quintic B-spline basis function.

For the simulation of the paralyzed patient, the system was modeled as an underactuated system with two actuated joints ($q_4$ and $q_5$) and five passive, or unactuated, joints ($q_6$, $q_7$, $q_8$, $q_9$, and $q_{10}$). The dynamics of such a hybrid dynamic system can be solved efficiently by the Lie group formulation discussed in [10]. In order to perform the optimization, an initial trajectory was required for the actuated joints. We used the trajectory identified from motion capture and defined it with the parameter set $P$ such that $q_a=q_a(t,P)$. Given the motion of the actuated joints, the dynamics of the partially actuated system were then integrated numerically from the given initial conditions using MATLAB's function "ode45," and our CSTORM dynamics software [10]. During the integration, the integral term in (9), $J_c=(1/2)\int_0^{t_f}\Sigma_{i=4}^{10} w_{ei}\tau_i^2 dt$, was also evaluated.

The steps taken above served to transform the optimal control problem (9) into the following discrete parameter optimization: Minimize $P$ subject to

$$J_{cp} = J_c + J_{p1} + J_{p2} + J_{p3} \quad (18)$$

$$H(q)\ddot{q} + h(q,\dot{q}) = \tau + \tau_{st} \quad (19)$$

$$p^0 = q_0, \quad p^1 = q_0 + \frac{1}{5}\dot{q}_0\Delta t \quad (20)$$

$$p^m = q_f, \quad p^{m-1} = q_f - \frac{1}{5}\dot{q}_f\Delta t \quad (21)$$

Note that the trajectory of the stance hip, $(q_1,q_2,q_3)$, was approximated as a B-spline curve based on the motion capture data. Equations (20) and (21) were used to meet the initial and final conditions (11) and (12), respectively. The actual variable parameters were $P$, excluding the fixed $p^0$, $p^1$, $p^{m-1}$, and $p^m$; and the total number of variable parameters was $n_a(m-3)$.

As described next, motions were generated by this dynamic motion optimization with different weighting coefficients for different cases. The weighting coefficients were chosen based on experience with many simulations. In each case, eight variable parameters ($m=11$) were used for each of the actuated joints. The joint torques were computed for the human model based on the estimated dynamic properties and the B-spline joint trajectories.

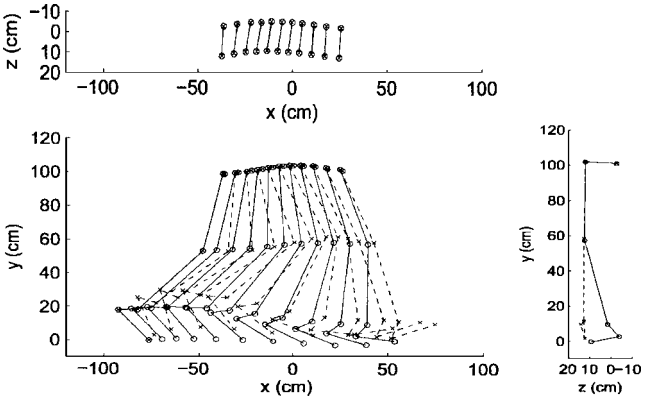


**Fig. 4 The resulting gait for Case 1: Paralyzed swing leg with motion captured stance hip orientation (no optimization). The solid lines show the resulting gait and the dashed lines are the gait recorded from the motion capture system.**

## 3 Results

We studied four different cases with the gait model, in order to gain insight into how robot motions applied at the pelvis might assist in gait generation:

- Case 1: Paralyzed swing leg with motion captured stance hip orientation (no optimization). This case was studied to determine if simply applying a normative pelvic trajectory would effectively control the swing leg.
- Case 2: Unimpaired swing leg with effort minimization of all joints. This case was studied to determine if the optimization technique produced realistic pelvic and leg trajectories when both the pelvis and the leg were assumed to be fully actuated.
- Case 3: Paralyzed swing leg with effort minimization of the stance hip torques. This case was studied to determine to what extent swing of a paralyzed leg could be controlled with pelvic motion alone.
- Case4: Paralyzed swing leg with effort minimization of the stance hip torques and bounded stance hip orientation. Case 3 produced large motions of the hip. Therefore, we sought to determine how limiting the hip motions affected the quality of swing control.

For these simulations, the stance and swing legs were the left and right legs, respectively.

**3.1 Case 1: Paralyzed Swing Leg With Motion Captured Stance Hip Orientation (No Optimization).** No optimization was applied in this case, in order to determine how the leg would swing if the pelvis were simply moved in a normative trajectory. The swing hip, knee, and ankle joints were set to be passive while the stance hip joint followed the trajectory identified from motion capture. Assuming no ground contact, the equations of motion were solved and the resulting motions are shown in Fig. 4. For clarity, the top $z$-$x$ view shows only the motion of the hip rotation centers. The front $y$-$z$ view shows only the final position of the swing leg. The dotted lines show the swing phase of the unimpaired right leg at a treadmill speed of 1.25 m/sec, as measured with the motion capture system. Note that the stance foot moved with the belt on the treadmill, however, for a clearer visualization of the swing leg movement, a constant-velocity transformation was applied to keep the stance foot fixed in this and subsequent plots. If contact with the ground was ignored, the swing leg attained a final configuration far from the desired one. Taking into account ground contact, the foot collided with the ground near the beginning of swing. As might be expected, this result demonstrates that simply replaying a desired pelvic trajectory does not effectively complete the swing motion of a paralyzed leg.

**Table 4 Weighting coefficients for cases 2, 3, 4. Note the high relative weighting on the penalty functions to ensure collision avoidance.**

| Case | $w_{e4}$, $w_{e5}$ | $w_{e6}$, $w_{e7}$, $w_{e8}$ | $w_{e9}$ | $w_{e10}$ | $w_{p1}$ | $w_{p2}$ | $w_{p31}$ | $w_{p32}$ |
|---|---|---|---|---|---|---|---|---|
| 2 | 0.05 | 0.05 | 0.1 | 2.5 | $5\times10^5$ | $5\times10^4$ | 0 | 0 |
| 3,4 | $10^{-4}$ | 0 | 0 | 0 | $10^5$ | $10^4$ | $10^3$ | $10^2$ |

**3.2 Case 2: Unimpaired Swing Leg With Effort Minimization of All Joints.** In order to test the ability of the optimization technique to mimic normal human control, we studied a fully actuated human model with actuated hip, knee, and ankle joints in the swing leg. A total of 56 parameters (parameters $p^2, p^3, \ldots, p^9$ for each actuated joint) were used in the optimization. The penalty functions that limited the allowable out of plane motion of the legs, $z_1$ and $z_2$ in $J_{p2}$, were chosen as

$$z_1(t) = z_{stance\text{-}hip}(t) + l_{hip} - 0.005 \tag{22}$$

$$z_2(t) = z_{stance\text{-}hip}(t) + l_{hip} - 0.033 \tag{23}$$

where $l_{hip}-0.005$ and $l_{hip}-0.033$ are the minimum horizontal distances (in meters) between the swing knee and the stance hip and between the swing heel and the stance hip, respectively, identified from motion capture. The weighting coefficients used for the optimization are listed in Table 4. They were chosen based on experience with many simulations. The large weighting of the penalty functions $w_{pi}$ impose a high cost if the legs collide with each other or with the ground. The optimization converged in 4 h of computation with a Pentium II-700 MHz PC. The resulting gait is shown in Fig. 5. The good correspondence with the human data suggests that human gait involves the minimization of effort. This effort/energy is applied to lift the swing leg to avoid contact with the ground and to achieve the final configuration. Moreover, the correspondence between the optimized and actual pelvic and leg joint motions suggests that the optimization technique can adequately predict what a normative trajectory would be, given only the limb dynamics and desired final configuration of the leg.

**3.3 Case 3: Paralyzed Swing Leg With Effort Minimization of the Stance Hip Torques.** To simulate a paralyzed person, the swing hip, knee, and ankle joints were made passive. A total of 16 parameters (parameters $p^2, p^3, \ldots, p^9$ for each actuated joint) were used in the optimization. The optimization took approximately 3.5 h to complete. The positions $z_1$ and $z_2$ in the penalty function $J_{p2}$ were chosen as

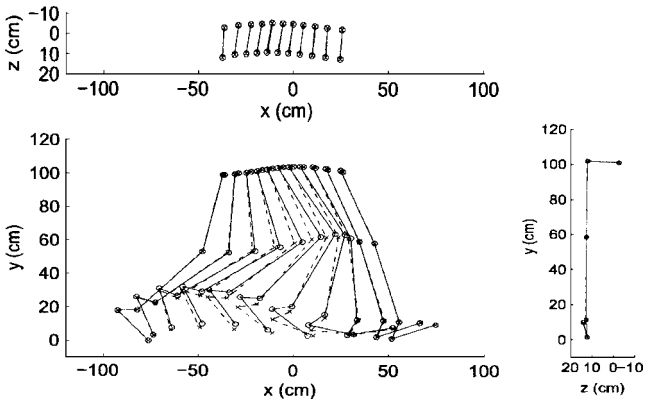


**Fig. 5 The resulting gait for case 2: Unimpaired swing leg. The solid lines show the resulting gait and the dashed lines are the gait recorded from the motion capture system.**

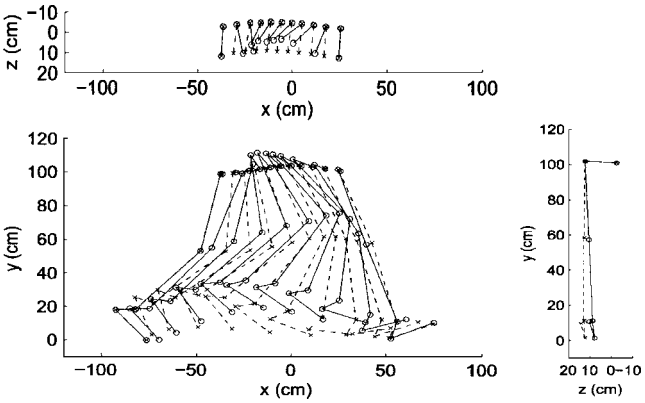


**Fig. 6 The resulting gait for case 3: Paralyzed swing leg. The solid lines show the resulting gait and the dashed lines are the gait recorded from the motion capture system.**

$$z_1(t) = z_2(t) = z_{stance\text{-}hip}(t) + \frac{2}{3}l_{hip} \tag{24}$$

in order to allow more hip adduction than the fully actuated case. The resulting motion is shown in Fig. 6. The optimizer lifted the swing hip to avoid collision between the swing leg and the ground. At the same time, it twisted the pelvis to pump energy into the paralyzed leg and moved the leg close to the desired final configuration, while avoiding collision between the legs. Thus, the optimizer was able to determine a strategy that could achieve repetitive stepping by shifting the pelvis alone. Note that the strategy incorporated a large swivel of the stance hip joint around the $y$ axis, which may be undesirable in step training a real human.

**3.4 Case 4: Paralyzed Swing Leg With Effort Minimization of the Stance Hip Torques and Bounded Stance Hip Orientation.** In order to determine if the large swivel motion in the previous case could be eliminated while still achieving a viable swing motion, we restricted the stance hip external/internal rotation within ±30° range by adding the following hard constraint to the optimization problem

$$-\frac{\pi}{6} \leqslant q_4 \leqslant \frac{\pi}{6} \tag{25}$$

The optimization took about 3.5 h to complete. The resulting gait is shown in Fig. 7, and demonstrates that a reasonable swing motion can be achieved while limiting excessive hip swivel.

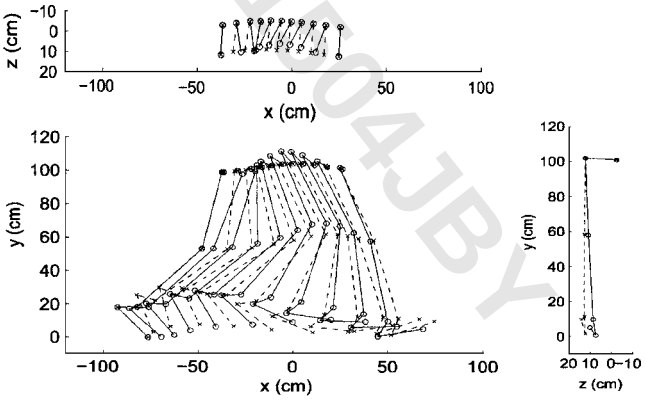


**Fig. 7 The resulting gait for case 4: Paralyzed swing leg with bounded stance hip orientation. The solid lines show the resulting gait and the dashed lines are the gait recorded from the motion capture system.**

**Table 5 The top rows show the peak torques (N m) about stance hip joint during motion for cases 1, 2, 3, and 4. The bottom rows show the joint position errors (degrees) in the swing leg from the trajectory of an unimpaired leg. $|q_f|$ is the absolute value of the error at the final position, and $|q(t)|_{avg}$ is the average absolute value of the error throughout the time interval.**

| | Case 1 | | Case 2 | | Case 3 | | Case 4 | |
|---|---|---|---|---|---|---|---|---|
| Joint | $\tau_{max}$ | $\tau_{min}$ | $\tau_{max}$ | $\tau_{min}$ | $\tau_{max}$ | $\tau_{min}$ | $\tau_{max}$ | $\tau_{min}$ |
| Stance hip ext/internal rotation ($\tau_4$) | 0 | 0 | 5.9 | −3.9 | 530.0 | −414.5 | 530.9 | −793.6 |
| Stance hip abduction/adduction ($\tau_5$) | 0 | 0 | −18.0 | −154.1 | 2884.3 | −2022.3 | 2576.0 | −3016.8 |
| | $\lvert q_f\rvert$ | $\lvert q(t)\rvert_{avg}$ | $\lvert q_f\rvert$ | $\lvert q(t)\rvert_{avg}$ | $\lvert q_f\rvert$ | $\lvert q(t)\rvert_{avg}$ | $\lvert q_f\rvert$ | $\lvert q(t)\rvert_{avg}$ |
| Swing hip abduction/adduction ($q_6$) | 10.7 | 2.0 | 0 | 3.0 | 2.7 | 18.2 | 2.8 | 14.3 |
| Swing hip ext/internal rotation ($q_7$) | 29.5 | 6.3 | 0 | 11.8 | 0.6 | 26.4 | 1.6 | 16.9 |
| Swing hip extension/flexion ($q_8$) | 1.2 | 11.9 | 0 | 2.4 | 4.1 | 11.3 | 2.3 | 6.3 |
| Swing knee extension/flexion ($q_9$) | 16.0 | 15.9 | 0 | 4.8 | 8.0 | 17.8 | 2.5 | 11.0 |
| Swing ankle plantar/dorsal flex ($q_{10}$) | 3.6 | 7.2 | 0 | 3.9 | 0.9 | 8.1 | 4.4 | 7.2 |

**3.5 Comparison of Cases.** As can be seen in Table 5, the fully actuated model in case 2 yielded the smallest final position error for the swing leg (zero error) compared to the other cases. However, the optimization technique produced a fairly small position error for case 3 (less than 5 deg on average across joints), indicating that the paralyzed leg could be driven via pelvic motion to a position from which stance might reasonably be initiated. Placing a limit on the amount of hip swivel did little to change the final position error of the paralyzed leg. In contrast, simply moving the pelvis along a motion-captured trajectory (i.e., case 1) created a relatively large final position error in the swing leg, even if the early ground contact during swing for this case was ignored.

The position errors of the swing leg compared to the motion capture data were not explicitly minimized throughout the trajectory, but it is interesting to compare these errors for the various cases ($|q(t)_{avg}|$ in Table 5). The fully actuated case again produced the smallest trajectory errors, which were on average about 5°, demonstrating the ability of the optimization technique to predict normative joint trajectories, even though only a final position error term was included in the cost function. The motion optimization technique for the underactuated cases (cases 3 and 4) produced larger trajectory errors than the motion-capture replay technique (case 1). This indicates that the motion optimization used moderately more "abnormal" stance hip and swing leg motions to achieve the desired leg configuration at heel strike. The toe did, however, contact the ground early during swing with simple motion replay, and this ground contact was ignored in calculating the trajectory error. The motions used to control the pelvis for the motion optimization cases avoided this ground collision.

## 4 Discussion and Conclusions

These results demonstrate the possible merits of incorporating robotic control of pelvic motion for use in step training with BWST. Although it may not be possible to fully control swing by manipulating the pelvis, the level of control that is possible appears sufficient for achieving reasonable swing trajectories and an approximate normal leg configuration at heel strike. This level of control should enable repetitive stepping on a treadmill by a completely paralyzed person. Further, the pelvic motions generated to control swing do not necessarily require large, nonphysiological joint movements.

The pelvic motion strategies generated by the optimizer are comparable to "hip hiking" gait strategies used by people with transfemoral lower limb prostheses [23], and by people with paralysis of one leg due to stroke [24]. In these strategies, the swing hip is lifted abnormally high in order to compensate for the lack of control at swing leg joints. This similarity suggests that the human nervous system itself may function like a motion optimizer as it finds solutions to underactuated control problems that are induced by injury [25]. Consistent with this concept, the human nervous system appears to function approximately as an effort minimizer during normal gait, as indicated by the good correspondence of the optimized and actual pelvic and leg trajectories in the fully actuated case. More complicated dynamic optimization studies of human locomotion that include detailed muscle models and seek to minimize metabolic cost have also found a good correspondence with normal gait [12,13]. The results of this study suggest that a simpler approach that minimizes joint effort without solving a tracking problem can also reproduce salient features of at least the swing phase of gait.

One possible limitation of the proposed control strategy is that a large peak hip abduction/adduction torque, almost 3000 Nm (Table 5), is required to create the desired motions. We are building a prototype robotic device [26] for manipulating the pelvis that makes use of high-force pneumatic actuators, but even so, it can generate at most approximately 1000 Nm of torque. Fortunately, however, the large torque is an artifact of the simplified model of the torso used in the simulations. Our model grouped the head, arms, and torso (HAT) into one rigid body. In order to rotate this rigid body about the $x$ axis of stance hip joint, a large torque is needed because the mass center of the HAT model is relatively far from the axis of rotation, and since the HAT is assumed to be rigid, the mass center moves in a circle about the rotation axis. This unrealistic circular motion requires the large torques. As suggested by [27], a better model of the HAT would include a "sacral-pelvic" joint in the lumbar region that allowed flexion/extension and lateral bending between the upper trunk and pelvis, plus an additional degree of freedom in the mid-thoracic region. The mass of the resulting pelvic segment would be approximately 80%–90% less than the combined HAT [28]. We estimated the torques that would be required to create the desired motions with such a modified model by moving the center of mass of our HAT segment into the lumbar region and decreasing the inertia by 1/5. The resulting required torques were an order of magnitude less, well within the bounds of our prototype robotic device, suggesting that creating the desired motions is feasible.

In this paper, we addressed the case in which the swing leg is flaccid. The goal of step training with BWST, however, is that the legs progress from a flaccid state to actively participating in stepping, by reprogramming locomotor control circuits within the spinal cord itself with appropriate patterns of sensory information. As the patient recovers stepping ability, the optimization technique outlined here could be repeated, taking into account the patterns of active forces applied by the patient's own muscles. These forces could be estimated given the dynamic model of the subject, knowledge of the forces applied by the robotic device, and measurements of the resulting limb motions. The motion optimization technique would then find the optimal motions for the specific

level of stepping ability for the patient. Such a strategy might also be useful in designing motions that can compensate for or accommodate mild, repeatable, spastic movements that sometimes occur following spinal cord injury. Of course, the presence of severe spasms would contraindicate the use of the control strategy outlined here. However, experienced step trainers report that such spasms are relatively infrequent if care is taken not to elicit inappropriate patterns of sensory input (e.g. nociceptive).

The results obtained in the optimization cases were local minimizers of the nonlinear cost function, although it would be more desirable to obtain globally minimizing motions. The algorithm was started with different initial trajectories in order to search for other minimizing motions, and several other solutions were found. The best of the trajectories (i.e., those with the smallest cost) are the results shown in this paper.

A pelvis-manipulating robot could also be useful for loading the stance leg by pressing downward on the stance hip, thus enhancing load-related sensory input used for stepping [29] at the same time as assisting in swing. An important goal for future research will be to determine how to couple force control of the stance leg with motion control of the swing leg.

More generally, dynamic motion optimization provides a useful tool for investigating novel strategies for assisting in locomotion rehabilitation. Finding strategies by observation of therapists is also desirable, but may miss some valuable strategies because therapists are limited in their control relative to robots. For example, the strategy found here requires hip torques that are quite large compared to a therapist's strength. Dynamic motion optimization also provides a formal means to automatically generate strategies on a patient-by-patient basis. Not only can patient-specific, gait-assisting motions be generated, but, based on the results from the fully actuated case, it also appears feasible to generate "normative" target motions using the principle of effort minimization for patients from whom this data cannot be measured.

## Acknowledgments

Thanks to Dana Craig of the Department of Veterans Affairs, Long Beach Healthcare System Prosthetics Gait Lab for assistance with the video capture data, and Christine Rose-Gottron of the Human Performance Laboratory at the UCI General Clinical Research Center for assistance with the active dynamometer data. Also, thanks to Dr. Susan Harkema and Dr. Reggie Edgerton for their helpful discussions regarding BWST. This investigation was supported by Public Health Service research grant M01 RR00827 from the National Center for Research Resources, and NIST Advanced Technology Program grant 00-00-4906.

## References

[1] Wickelgren, I., 1998, "Teaching the Spinal Cord to Walk," Science, **279**, pp. 319–321.

[2] Behrman, A., and Harkema, S., 2000, "Locomotor Training after Human Spinal Cord Injury: A Series of Case Studies," Phys. Ther., **80**, pp. 688–700.

[3] Barbeau, H., Norman, K., Fung, J., Visintin, M., and Ladoucer, M., 1998, "Does Neurorehabilitation Play a Role in the Recovery of Walking in Neurological Populations," Ann. N.Y. Acad. Sci., **860**, pp. 377–392.

[4] Hesse, S., Uhlenbrock, D., and Sarkodie-Gyan, T., 1999, "Gait Pattern of Severely Disabled Hemiparetic Subjects on a New Controlled Gait Trainer as Compared to Assisted Treadmill Walking with Partial Body Weight Support," Clin. Rehabil., **13**, pp. 401–410.

[5] Hesse, S., and Uhlenbrock, D., 2000, "A Mechanized Gait Trainer for Restoration of Gait," J. Rehabil. Res. Dev., **37**(6), pp. 701–708.

[6] Colombo, G., Joerg, M., Schreier, R., and Dietz, V., 2000, "Treadmill Training of Paraplegic Patients with a Robotic Orthosis," J. Rehabil. Res. Dev., **37**(6), pp. 693–700.

[7] Reinkensmeyer, D. J., Wynne, J. H., and Harkema, S. J., 2002, "A Robotic Tool for Studying Locomotor Adaptation and Rehabilitation," *Proceedings of the Second Joint Meeting of the IEEE Engineering in Medicine and Biology Society and the Biomedical Engineering Society*, 3, pp. 2353–2354.

[8] Bejczy, A., 1999, "Towards Development of Robotic Aid for Rehabilitation of Locomotion-Impaired Subjects," *Proceedings of the First Workshop on Robot Motion and Control (RoMoCo'99)*, pp. 9–16.

[9] Albro, J. V., Sohl, G. A., Bobrow, J. E., and Park, F. C., 2000, "On the Computation of Optimal High-Dives," *IEEE International Conference on Robotics and Automation*, 4, pp. 3958–3963.

[10] Sohl, G. A., and Bobrow, J. E., 2001, "A Recursive Multibody Dynamics and Sensitivity Algorithm for Branched Kinematic Chains," ASME J. Dyn. Syst., Meas., Control, **123**(3), pp. 391–399.

[11] Hodgins, J. K., 1996, "Three-Dimensional Human Running," *IEEE International Conference on Robotics and Automation*, 4, pp. 3271–3276.

[12] Pandy, M. G., and Anderson, F. C., 2000, "Dynamic Simulation of Human Movement Using Large-Scale Models of the Body," *IEEE International Conference on Robotics and Automation*, 1, pp. 676–681.

[13] Anderson, F. C., and Pandy, M. G., 2001, "Dynamic Optimization of Human Walking," J. Biomech. Eng., **123**(5), pp. 381–390.

[14] Wang, C-Y. E., Bobrow, J. E., and Reinkensmeyer, D. J., 2001, "Swinging from the Hip: Use of Dynamic Motion Optimization in the Design of Robotic Gait Rehabilitation," *IEEE International Conference on Robotics and Automation*, 2, pp. 1433–1438.

[15] Thorstensson, A., Nilsson, J., Carlson, H., and Zomlefer, MR., 1984, "Trunk Movements in Human Locomotion," Aeronaut. Q., **121**(1), pp. 9–22.

[16] Bell, A. L., Brand, R. A., and Pedersen, D. R., 1989, "Prediction of Hip Joint Centre Location From External Landmarks," Hum. Mov. Sci., **8**, pp. 3–16.

[17] Kirkwood, R. N., Culham, E. G., and Costigan, P., 1999, "Radiographic and Non-invasive Determination of the Hip Joint Center Location: Effect on Hip Joint Moments," Clin. Biomech. (Los Angel. Calif.), **14**(4), pp. 227–235.

[18] Zatslorsky, V., and Seluyanov, V., 1985, "Estimation of the Mass and Inertia Characteristics of the Human Body by Means of the Best Prediictive Regression Equations," *Biomechanics IX-B*, D. A. Winter et al. eds., Human Kinetics Publishers, Champain, Illinois, pp. 233–239.

[19] Dempster, W. T., and Gaughran, G. R. L., 1968, "Properties of Body Segments Based on Size and Weight," Am. J. Anat., **120**, pp. 33–54.

[20] Bartels, R. H., Beatty, J. C., and Barsky, B. A., 1987, *An Introduction to Splines for Use in Computer Graphics and Geometric Modeling*, Morgan Kaufmann, Las Altos, CA.

[21] Wang, C-Y. E., Timoszyk, W. K., and Bobrow, J. E., 1999, "Weightlifting Motion Planning for a Puma 762 robot," *IEEE International Conference on Robotics and Automation*, 1, pp. 480–485.

[22] Wang, C-Y. E., Timoszyk, W. K., and Bobrow, J. E., 2001, "Payload Maximization for Open Chained Manipulators: Finding Weightlifting Motions for a Puma 762 Robot," IEEE Trans. Rob. Autom., **17**(2), pp. 218–224.

[23] Michaud, S. B., Gard, S. A., and Childress, D. S., 2000, "A Preliminary Investigation of Pelvic Obliquity Patterns During Gait in Persons with Transtibal and Transfemoral Amputation," J. Rehabil. Res. Dev., **37**(1), pp. 1–10.

[24] Kerrigan, D. C., Frates, E. P., Rogan, S., and Riley, P. O., 2000, "Hip Hiking and Circumduction: Quantitative Definitions," Am. J. Phys. Med. Rehabil., **79**(3), pp. 247–252.

[25] Latash, M. L., and Anson, J. G., 1996, "What are Normal Movements in Atypical Populations?," Behav. Brain Res., **19**(1), pp. 55–106.

[26] Ichinose, W. E., Reinkensmeyer, D. J., Aoyagi, D., Lin, J. T., Ngai, K., Edgerton, V. R., Harkema, S. J., and Bobrow, J. E., "A Robotic Device for Measuring and Controlling Pelvic Motion During Locomotor Rehabilitation," *Proceedings of the 2003 IEEE Engineering in Medicine and Biology Society Meeting*.

[27] Yamaguchi, G., 1990, "Performing Whole-Body Simulations of Gait with 3-D, Dynamic Musculoskeletal Models," *Multiple Muscle Systems: Biomechanics and Movement Organization*, J. M. Winters and S. L-Y. Woo ed., Springer Verlag, pp. 663–679.

[28] Erdmann, W. S., 1997, "Geometric and Inertial data of the trunk in adult males," J. Biomech., **30**(7), pp. 679–688.

[29] Harkema, S. J., Hurley, S. L., Patel, U. K., Requejo, P. S., Dobkin, B. H., and Edgerton, V. R., 1997, "Human Lumbosacral Spinal Cord Interprets Loading During Stepping," J. Neurophysiol., **77**(3), pp. 797–811.